Available online at www.sciencedirect.com
ScienceDirect
Journal of Power Sources 176 (2008) 403–409
JOURNAL OF POWER SOURCES
www.elsevier.com/locate/jpowsour

Preparation and enhanced capacitance of core–shell polypyrrole/polyaniline composite electrode for supercapacitors

Hongyu Mi [a,b], Xiaogang Zhang [c,*], Xiangguo Ye [a], Sudong Yang [a]

[a] *Institute of Applied Chemistry, Xinjiang University, Urumqi 830046, PR China*
[b] *College Science of Xi'an Jiaotong University, Xi'an 710049, PR China*
[c] *College of Material Science & Engineering, Nanjing University of Aeronautics and Astronautics, Nanjing 210016, PR China*

Received 28 July 2007; received in revised form 18 October 2007; accepted 23 October 2007
Available online 30 October 2007

Abstract

Polypyrrole (PPy) nanotubes were synthesized by using the complex of methyl orange (MO)/$FeCl_3$ as a template. Then the core–shell polypyrrole/polyaniline (PPy/PANI) composite was prepared by *in situ* chemical oxidation polymerization of aniline on the surface of PPy nanotubes. The morphology and molecular structure were characterized by transmission electron microscopy (TEM), infrared spectroscopy (IR) and X-ray diffraction (XRD). TEM images confirmed that the composite was core–shell nanotubes. The electrochemical properties of the PPy/PANI composite electrode were investigated by cyclic voltammetry (CV), galvanostatic charge–discharge and electrochemical impedance spectroscopy (EIS). The electrochemical experiments showed that the specific capacitance of the PPy/PANI composite was 416 F g^{-1} in 1 M H_2SO_4 electrolyte and 291 F g^{-1} in 1 M KCl electrolyte. Furthermore, the composite electrode exhibited a good rate capability and maintained 91% of initial capacity at a current density of 15 mA cm^{-2} in 1 M H_2SO_4 electrolyte.

Keywords: Core–shell structure; Polypyrrole/polyaniline composite; Supercapacitor

1. Introduction

Electrochemical supercapacitors are a kind of energy-storage devices between conventional capacitors and batteries, which have various applications in electric vehicles, cellular communication devices, portable computers and nano-electronics [1–4]. Based on the charge-storage mechanism, supercapacitor can be classified into two categories: (1) electrochemical double-layer capacitors, which is derived from charge separation; (2) redox capacitors, which is due to the redox reactions through the volume of the material rather than just at the outer surface of particles [5]. In general, the energy density of redox capacitors consisting of transition metal oxides and conducting polymers is higher than that of double-layer capacitors composed of carbon materials. Hence, more and more researchers focused on studying the synthesis and electrochemical properties of electrically conducting polymers (ECPs) including polyaniline, polypyrrole, polythiophene and their derivatives, which represent promising electrode materials for the application of supercapacitors due to their high specific capacitance [6–12]. However, these conducting polymers are used in different electrolytes to obtain a higher specific capacitance, for example, the favored electrolytes for polyaniline are usually acidic solution [6,13,14], whereas polypyrrole and polythiophene exhibit ideally capacitance behavior in neutral and basic electrolytes [15–17]. Therefore, to develop the composite electrode material for supercapacitors is a possible route to satisfy the requirements of technology application in different medium. Very recently, Xu et al. [18] reported the synthesis of poly(3,4-ethylenedioxythiophene)/polypyrrole composite, and proved that the composite was an ideal electrode material in 1 M KCl electrolyte.

In this work, the core–shell PPy/PANI composite was successfully achieved by *in situ* polymerization of aniline on the surface of PPy nanotubes. More important aim was to obtain a new composite electrode with good electrochemical performance in both acidic and neutral electrolytes. Therefore, its capacitive behavior in two electrolytes was systematically

* Corresponding author. Tel.: +86 25 52112902; fax: +86 25 52112626.
E-mail address: azhangxg@163.com (X. Zhang).

0378-7753/$ – see front matter © 2007 Elsevier B.V. All rights reserved.
doi:10.1016/j.jpowsour.2007.10.070

examined by cyclic voltammetry (CV), galvanostatic charge–discharge and electrochemical impedance spectroscopy (EIS). The results showed that the PPy/PANI composite had potential application for supercapacitors in the acidic and neutral electrolytes due to the combination of the complementary properties of PPy and PANI.

2. Experimental

2.1. Materials

Aniline (AN, analytical purity, Beijing Chemical Reagent Co., China) and pyrrole monomer (Py, 99%, Aldrich chemical Co.) were purified through distillation under reduced pressure and stored refrigerated before use. All other chemicals including ferric chloride ($FeCl_3$), ammonium persulfate ($(NH_4)_2S_2O_8$, APS) and methyl orange (MO), were analytical purity and used as received without further treatment. All the solutions were prepared using de-ionized water.

2.2. Synthesis of PPy nanotubes and PPy/PANI composite

The PPy/PANI composite was prepared by two-step procedure. The synthesis of PPy nanotubes used as the template in this work was similar to the literature [19]. The difference between the two syntheses was that the reaction condition in our experiment was under static condition in a lower temperature. In a typical process, an appropriate amount of $FeCl_3$ was dissolved in 5 mM methyl orange (MO) de-ionized water solution (60 mL). A flocculent precipitate appeared immediately. After stirring for 30 min, 210 μL pyrrole was slowly added into the above solution in 10 min, and then left under static condition for 24 h at −5 °C. The black precipitate was filtered and washed with de-ionized water and ethanol, then dried under vacuum for 24 h at 50 °C.

The PPy/PANI composite was prepared by *in situ* chemical oxidation polymerization according to the following steps. 0.05 g PPy nanotubes was dispersed in 0.2 M H_2SO_4 (45 mL) and ultrasonicated for 15 min, then transferred into an ice-bath. 5 mmol aniline monomer was added to the above suspension and further stirred for 30 min so that aniline was uniformly adsorbed on the surfaces of PPy. 0.2 M H_2SO_4 (5 mL) containing 1.14 g APS was slowly added dropwise into the suspension in 10 min with constant mechanical stirring. The reaction was carried out under static condition for an additional 24 h at −5 °C. The resulting dark green suspension was obtained after filtration, washing and drying under the same condition.

2.3. Structure characterization

The TEM images were obtained by using a Hitachi-600 microscope. Infrared spectra (IR) were obtained with BRUKER-EQUINOX-55 IR spectrometer in the range of 3500–500 cm^{-1}. The samples were prepared in KBr pellets. The X-ray powder diffraction (XRD) patterns of the obtained samples were characterized by using the M18X^{ce} X-ray diffractometer with Cu Kα radiation (λ = 0.154056 nm), employing a scanning rate of 10° min^{-1} in the 2θ range of 5–60°.

2.4. Electrochemical tests

The electrode of the PPy/PANI composite was prepared by mixing 85 wt.% active materials (3 mg), 10 wt.% carbon black and 5 wt.% polytetrafluoroethylene (PTFE). Then the mixture was pressed on the graphite electrode (1 cm^2) as a current collector. Subsequently, the electrode was dried at 50 °C for 4 h before use. The PPy and PANI electrodes were also prepared according to the above procedure, and the mass load of every sample is 3 mg. The electrolytes were 1 M H_2SO_4 and 1 M KCl.

The electrochemical behavior of the composite electrode was evaluated by cyclic voltammetry (CV), galvanostatic charge–discharge and electrochemical impedance spectroscopy (EIS) techniques. All electrochemical experiments were carried out in a three-electrode glass cell, a platinum counter electrode, and a standard calomel reference electrode (SCE). CV and galvanostatic charge–discharge tests were performed in the potential window ranged from −0.2 to 0.8 V (vs. SCE) using a CHI660A electrochemical working station. EIS measurements were performed at open-circuit potential by using an AUTO-

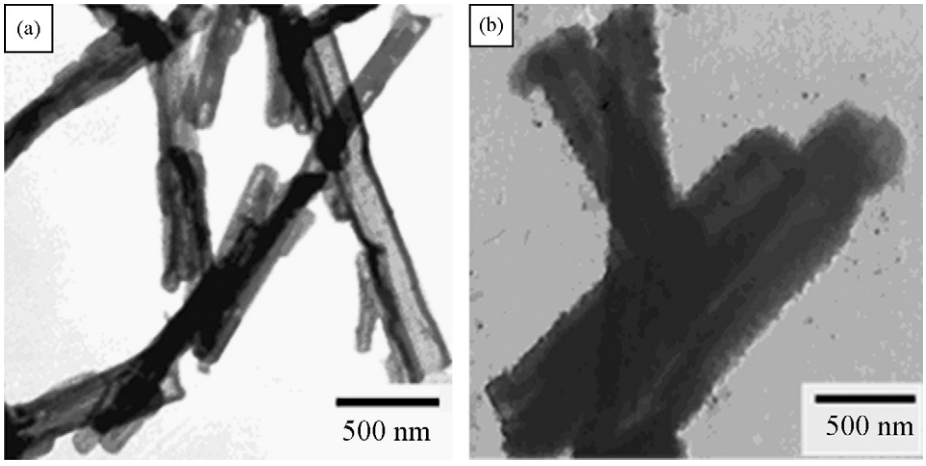

Fig. 1. TEM images of (a) PPy and (b) PPy/PANI composite.

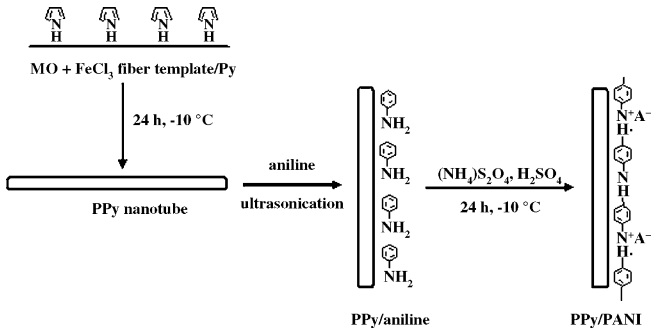

Fig. 2. Polymerization of pyrrole and preparation of PPy/PANI composite.

LAB PGSTAT30. Data were collected in the frequency range of 10^{-2} to 10^{5} Hz.

3. Results and discussion

3.1. Morphology and formation process

Fig. 1 shows the TEM images of PPy and PPy/PANI composite. It was clear that PPy was nanotube shape and about 150–300 nm in diameter (Fig. 1a). However, it was observed in Fig. 2b that the composite was the typical core–shell structure, and PPy acted as the "core" via the hard template. The aniline monomer was uniformly polymerized on the surface of PPy and formed a shell of the composite. From Fig. 1b, it can be evaluated that the diameter of the composite was around 300–500 nm. According to the TEM images, the possible formation process of the composite is given in Fig. 2.

The IR spectra of PPy, PANI and PPy/PANI composite are presented in Fig. 3. The main characteristic peaks of PPy were assigned as follows: the bands at 1540 and 1446 cm^{-1} were attributed to the pyrrole ring vibration. The bands located at 1305 and 1090 cm^{-1} were ascribed to the =C–H in-plane deformation, while other bands at 1156 and 964 cm^{-1} reflected the C–N stretching vibration and the =C–H out-of-plane vibration, respectively. The results were in agreement with the literature values [19,20]. The peaks of PANI at 1575, 1491, 1297 and 1108 cm^{-1} corresponded to C–C stretching mode of the

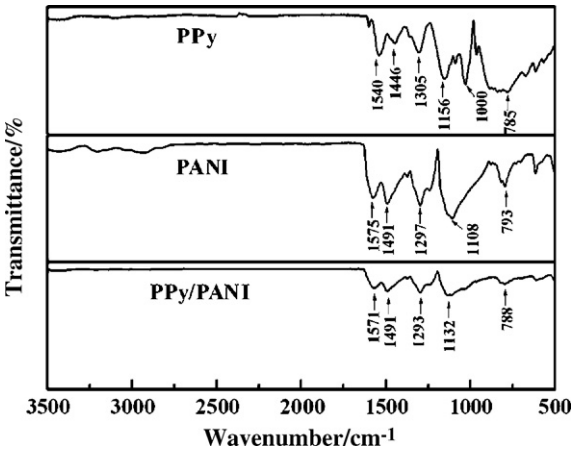

Fig. 3. IR spectra of PPy, PANI and PPy/PANI composite.

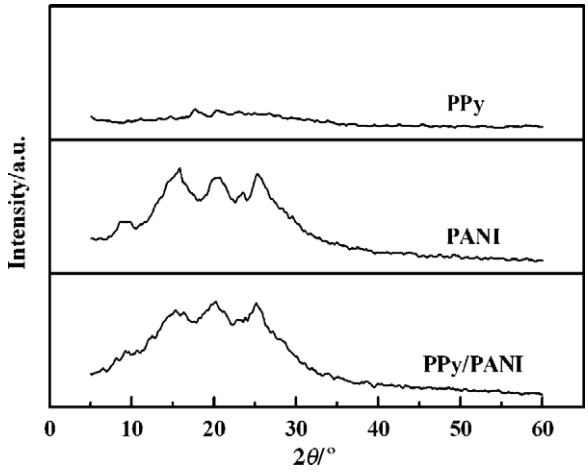

Fig. 4. XRD patterns of PPy, PANI and PPy/PANI composite.

quinoid rings, C=C stretching mode of the benzenoid rings, C–N stretching mode and N=Q=N (Q represents the quinoid ring), respectively. Compared with the corresponding characteristic peaks of PPy and PANI, it could be evidently seen from Fig. 3 that IR spectrum of the PPy/PANI composite reflected the mutual influence of PANI and PPy. But some spectroscopic differences in the peak intensity and position revealed that there was interaction between PANI and PPy instead of a simple blend of the two polymers.

Fig. 4 shows the X-ray diffraction patterns of PPy, PANI and PPy/PANI composite. The XRD pattern of PPy exhibited the broad and weak reflection located in the range of 15–30°, which were the characteristic peak of amorphous PPy. However, in the XRD pattern of PANI, several peaks centered at $2\theta = 5°$, 21° and 25° were ascribed to the periodicity parallel and perpendicular to the polymer chains of PANI, respectively [21]. This indicated that PANI had higher crystalline in comparison with PPy. For the PPy/PANI composite, it had a similar structure to PANI, implying that amorphous PPy had indistinctive effect on the crystal structure of PANI. So, it suggested that the crystalline of the composite was enhanced by the introduction of PANI. It was a possible reason that, when PANI was adhered to PPy via polymerization of aniline on the surface of amorphous PPy, the molecular chain of PANI was confined.

To evaluate the electrochemical characteristics of the electrode for supercapacitors, current–potential response was employed to investigate the effect of the electrolyte on the electrochemical performance at the potential window from −0.2 to 0.8 V versus SCE. Fig. 5 illustrates the CV curves of PPy, PANI and PPy/PANI composite electrodes measured in 1 M H_2SO_4 electrolyte and 1 M KCl electrolyte at a scan rate of 5 mV s^{-1}. From Fig. 5a and b, some important information could be noticed. The CV curves of PPy were similar in the acidic and neutral electrolytes, and revealed a little deviation from a rectangular form, whereas some considerable differences were observed for the PPy/PANI composite electrode in the two electrolytes. The peak currents of the composite in acidic electrolyte were relatively higher than those in neutral electrolyte, implying that the specific capacitance of the composite in acidic

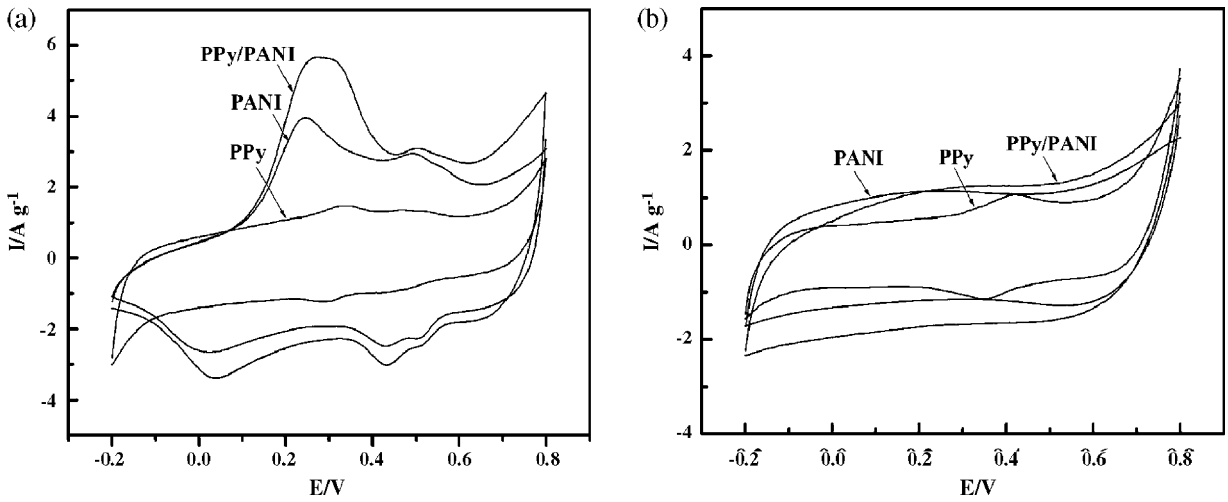

Fig. 5. CV curves of PPy, PANI and PPy/PANI composite electrodes at 5 mV s^{-1} in (a) 1 M H_2SO_4 electrolyte and (b) 1 M KCl electrolyte. Mass of the active material in every sample: 3 mg.

electrolyte was greater than that in neutral electrolyte owing to the participance of PANI. Although the CV shapes of the composite in the two electrolytes were similar to those of PANI (Fig. 5), the peak currents for the composite were higher compared with those for PANI. This improvement in current may be ascribed to the special nanostructure of this composite. Based on the above analysis, the composite was more available for use in the acid electrolyte because the higher specific capacitance could be obtained in this electrolyte. However, it was well known that the electrode material was more applicable and extensive for the application of supercapacitors in the neutral medium [18,22]. Thus, in order to match the requirement of the application in supercapacitors, it was very essential to study the electrochemical properties of electrode materials in the neutral medium.

In order to further research the properties of the PPy/PANI composite electrode, Fig. 6 shows the CV curves of the composite electrode at scan rates of 10, 20 and 30 mV s^{-1}. In Fig. 6a, three pairs of redox peaks (P_1/P_2, P_3/P_4 and P_5/P_6) can be found. They were attributed to the redox process of PANI on PPy nanotubes. Peak P_1/P_2 (0.35/−0.03 V) was assigned as the redox transition of PANI between a semi-conductive state and a conducting state. Peak P_3/P_4 (0.65/0.4 V) was due to the formation of the *p*-benzoquinone/hydroquinone couple [23,24]. Peak P_5/P_6 (0.8/0.6 V) was ascribed to the formation/reduction of bipolaronic pernigraniline and protonated quinonediimine [23–25]. With the increase of a scan rate from 10 to 30 mV s^{-1}, the peak current (P_1) rapidly increased from 10 to 19 A g^{-1}, indicating a good rate ability of the composite electrode in acidic solution. The same result was also seen in Fig. 6b, in which the current increased to some extent as the scan rate increased.

Fig. 7 gives the galvanostatic charge–discharge curves of PPy, PANI and PPy/PANI composite electrode examined in 1 M H_2SO_4 electrolyte and 1 M KCl electrolyte at a current density of 3 mA cm^{-2}. The specific capacitance (C_m) can be calculated

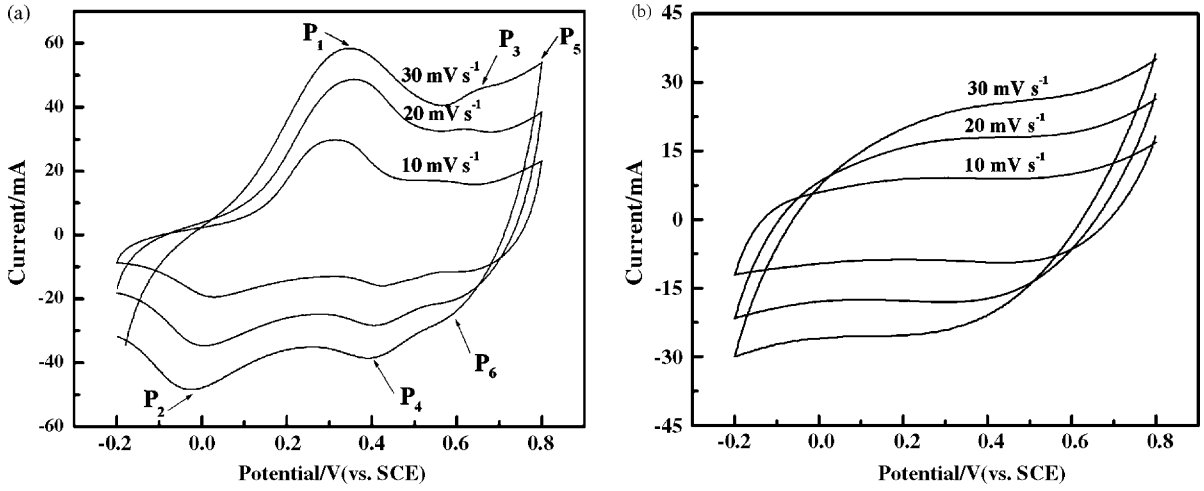

Fig. 6. CV curves of PPy/PANI composite electrode at various scan rates in (a) 1 M H_2SO_4 electrolyte and (b) 1 M KCl electrolyte. Mass of the active material: 3 mg.

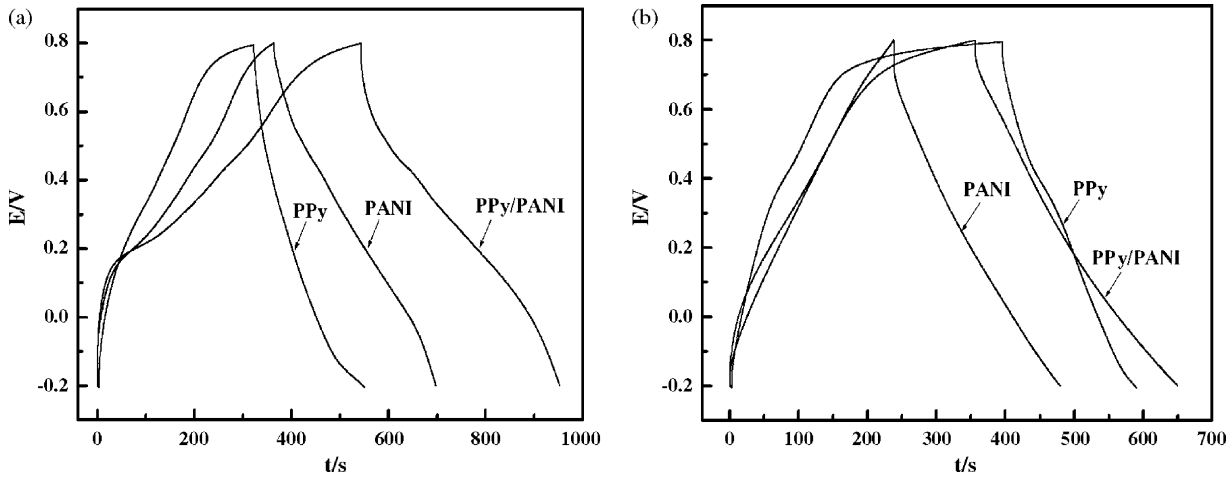

Fig. 7. Galvanostatic charge–discharge curves of PPy, PANI and PPy/PANI composite electrode at a current density of 3 mA cm^{-2} in (a) 1 M H_2SO_4 electrolyte and (b) 1 M KCl electrolyte. Mass of the active material in every sample: 3 mg.

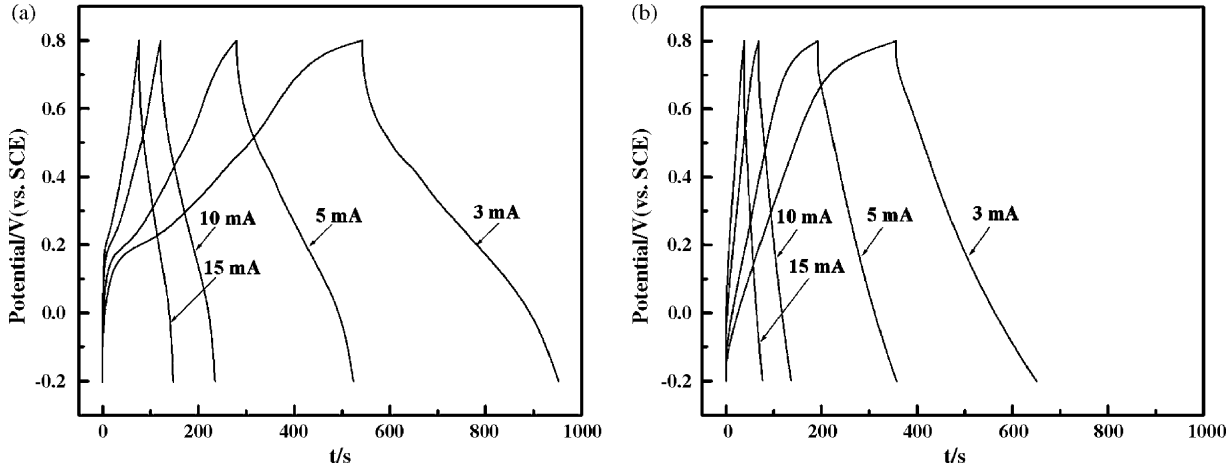

Fig. 8. Galvanostatic charge–discharge curves of PPy/PANI composite electrode at current density of 3, 5, 10 and 15 mA cm^{-2} in (a) 1 M H_2SO_4 electrolyte and (b) 1 M KCl electrolyte. Mass of the active material: 3 mg.

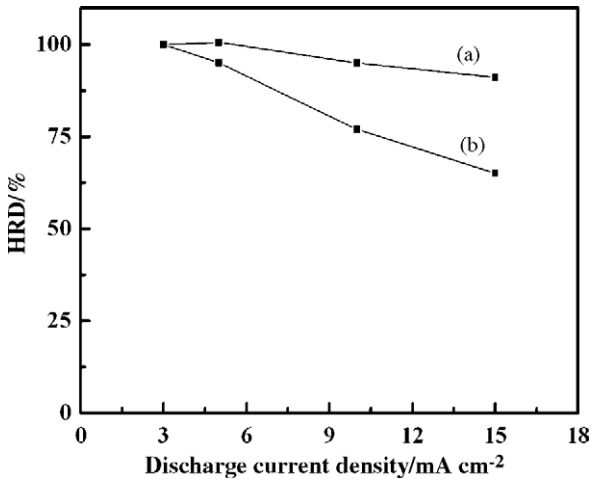

Fig. 9. High-rate dischargeability (HRD) for PPy/PANI composite electrode in (a) 1 M H_2SO_4 electrolyte and (b) 1 M KCl electrolyte. Mass of the active material: 3 mg.

according to Eq. (1):

$$C_m = \frac{C}{m} = \frac{I\Delta t}{\Delta V m} \quad (1)$$

where I is the charge–discharge current, Δt is the discharge time, ΔV is the electrochemical window (1 V), and m is the mass of active material within the electrode (3 mg). The specific capacitances of PPy, PANI and PPy/PANI composite calculated from Fig. 7a were 230, 336 and 416 F g^{-1} at 3 mA cm^{-2}, respectively. While the corresponding values from Fig. 7b were 197, 244 and 291 F g^{-1}.

Table 1
The specific capacitances of the PPy/PANI composite electrode evaluated according to Eq. (1) at various current densities

	Current density (mA cm^{-2})			
	3	5	10	15
C_m (F g^{-1}) in acidic electrolyte	416	419	394	378
C_m (F g^{-1}) in neutral electrolyte	291	275	223	189

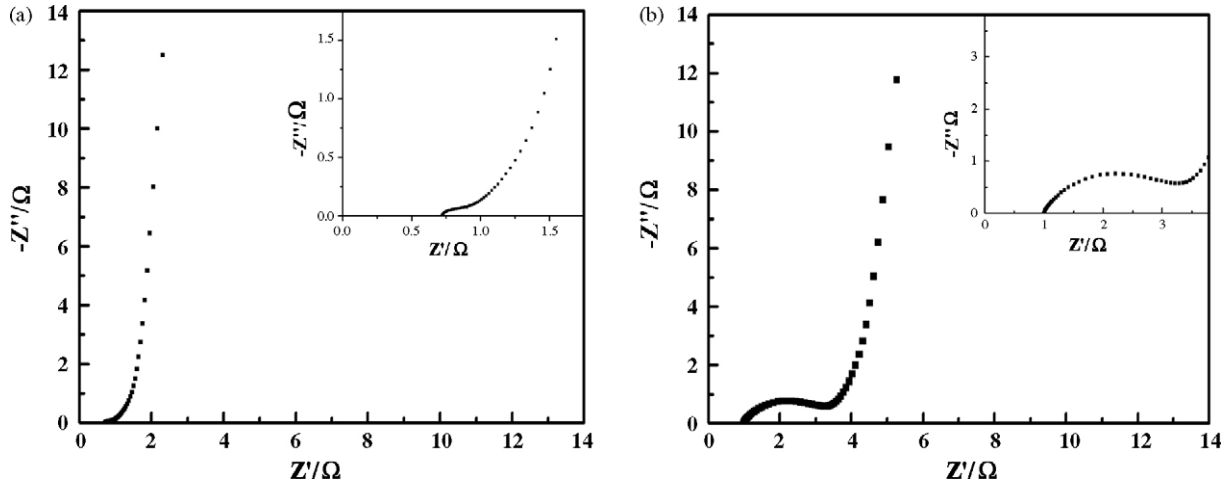

Fig. 10. The Nyquist plots of PPy/PANI composite electrodes in (a) 1 M H_2SO_4 electrolyte and (b) 1 M KCl electrolyte. Mass of the active material: 3 mg.

Fig. 8 displays galvanostatic charge–discharge curves of the PPy/PANI composite electrode at current densities of 3, 5, 10 and 15 mA cm^{-2}. In Fig. 8a, the curves behaving a mirror-like during the charge–discharge process at various current densities meant that the PPy/PANI composite electrode owned better electrochemical capacitance performance in acidic electrolyte compared with that in neutral electrolyte (Fig. 8b), which was consistent with the result of CV test. And the calculated results are listed in Table 1. The discharge capacitance of the PPy/PANI composite electrode decreased along with the increase of charge–discharge current densities, which was responsible to the internal resistance and polarization of the electrode [26]. The largest specific capacitance was 419 F g^{-1} at 5 mA cm^{-2} in 1 M H_2SO_4 electrolyte, and 291 F g^{-1} in 1 M KCl electrolyte at 3 mA cm^{-2}. So this composite electrode was more favorable for the applications of supercapacitors in low current density. It is significant for the electrode material that can afford the higher specific capacitance. Moreover, the composite electrode had a good rate capability in the acidic electrolyte. The specific capacitance decreased from 416 to 378 F g^{-1} when the current density increased from 3 to 15 mA cm^{-2}. It only lost 9% of the initial specific capacitance even in the charge–discharge current density up to 15 mA cm^{-2}. The above studies proposed that the composite electrode had a fast redox process, leading to good power ability.

To compare the power properties of the composite electrode in different electrolytes, the high-rate dischargeability (HRD) of the electrode was also employed. The HRD can be obtained using Eq. (2):

$$\mathrm{HRD}(\%) = \frac{C_d}{C_1} \times 100 \quad (2)$$

where C_d and C_1 are the discharge capacity of electrodes at a certain current density and 1 mA cm^{-2}, respectively.

Fig. 9 shows the relationship between the high-rate dischargeability and the discharge current density. It was clear from Fig. 9 that the specific capacitance decreased with increasing current density due to the internal resistance of the electrode. The composite electrode exhibited better HRD in 1 M H_2SO_4 electrolyte, deducing that the power characteristic of this electrode was improved in the acidic electrolyte.

Furthermore, the electrochemical impedance spectroscopy was also carried out to prove the capacitive performance at the open-circuit potential in the frequency range of 0.01–10^5 Hz with ac-voltage amplitude of 5 mV. The typical Nyquist plots of PPy/PANI composite electrode are given in Fig. 10. Firstly, in high frequency intercept of the real axis, an internal resistance (R_s) can be observed, which included the resistance of the electrolyte, the intrinsic resistance of the active material, and the contact resistance at the interface active material/current collector. Its value was approximately 0.7 Ω in 1 M H_2SO_4 and 1 Ω in 1 M KCl electrolyte. Secondly, in the medium-to-low frequency region, the unequal semicircular can be discovered in different electrolytes, as shown in the up-right corner of Fig. 10. The radius of the semicircular in 1 M H_2SO_4 electrolyte was smaller than that in 1 M KCl electrolyte. Herein, the charge-transfer resistance was smaller in the acidic electrolyte. In low frequency, the impedance plots exhibited a slightly tilted vertical line of a limiting diffusion process in two electrolytes, which was characteristic feature of pure capacitive behavior [27].

4. Conclusions

In this paper, the core–shell PPy/PANI composite with an average diameter of 300–500 nm was prepared by the polymerization of aniline on the surface of PPy nanotubes. The electrochemical proprieties of the composite as an active electrode material were in detail investigated in two different electrolytes by a series of electrochemical techniques. The results showed that the specific capacitance of the composite was 416 F g^{-1}, approximately 40% larger than that in the acidic electrolyte (291 F g^{-1}). At the same time, the composite electrode showed a good rate capability in the acidic electrolyte, and it only lost 9% of the initial specific capacitance with the charge–discharge current density up to 15 mA cm^{-2}.

Acknowledgments

The work was supported by National Basic Research Program of China (973 Program) (no. 2007CB209703), Natural Sciences Foundation of China (nos. 20403014 and 206330400) and Natural Sciences Foundation of Jiangsu Province (BK2006196).

References

[1] B.E. Conway, W. Pell, Proceedings of the 8th International Seminar on Double-Layer Capacitors and Similar Energy-Storage Devices, Florida Educational Seminars, Deerfield Beach, FL, December 7–9, 1998.
[2] C. Arbizzani, M. Mastragostino, B. Scosati, in: H.S. Nalwa (Ed.), Handbook of Organic Conductive Molecules and Polymers, vol. 4, Wiley, Chichester, UK, 1997, p. 595.
[3] S. Sarangapani, B.V. Tilak, C.P. Chen, J. Electrochem. Soc. 143 (1996) 3791–3799.
[4] K. Lota, V. Khomenko, E. Frackowiak, J. Phys. Chem. Solids 65 (2004) 295–301.
[5] A. Rudge, I. Raistrick, S. Gottesfeld, J.P. Ferraris, Electrochim. Acta 39 (1994) 273–287.
[6] K.S. Ryu, K.M. Kim, S.G. Kang, J. Joo, S.H. Chang, J. Power Sources 88 (2000) 197–201.
[7] D. Belanger, X. Ren, J. Davey, F. Uribe, S. Gottesfeld, J. Electrochem. Soc. 147 (2000) 2923–2929.
[8] F. Fusalba, P. Gouerec, D. Villers, D. Belanger, J. Electrochem. Soc. 148 (2001) A1–A6.
[9] K.R. Prasad, N. Munichand, J. Power Sources 112 (2002) 443–451.
[10] K.R. Prasad, N. Miura, J. Power Sources 134 (2004) 354–360.
[11] V. Gupta, N. Miura, J. Power Sources 157 (2006) 616–620.
[12] A. Laforgue, P. Simon, C. Sarrazin, J.F. Fauvarque, J. Power Sources 80 (1999) 142–148.
[13] A. Mirmohseni, R. Solhjo, Eur. Polym. J. 39 (2003) 219–223.
[14] V. Gupta, N. Miura, Electrochem. Solid-State Lett. 8 (12) (2005) A630–A632.
[15] C. Arbizzani, M. Mastragostino, L. Menegheta, Electrochim. Acta 41 (1996) 21–26.
[16] A. Rudge, I. Raistrick, S. Gottesfeld, J.P. Ferraris, J. Power Sources 47 (1994) 89–107.
[17] F. Fusalba, N. E1 Mehdi, L. Breau, D. Belanger, Chem. Mater. 11 (1999) 2743–2753.
[18] J. Wang, Y.L. Xu, X. Chen, X.F. Du, J. Power Sources 163 (2007) 1120–1125.
[19] X.M. Yang, Z.X. Zhu, T.Y. Dai, Y. Lu, Macromol. Rapid Commun. 26 (2005) 1736–1740.
[20] J. Liu, M.X. Wan, J. Polym. Sci., A: Polym. Chem. 39 (2001) 997–1004.
[21] L. Zhang, Synth. Met. 156 (2006) 454–458.
[22] C.-C. Hu, J.-Y. Lin, Electrochim. Acta 47 (2002) 4055–4067.
[23] C.-C. Hu, C.-H. Chu, J. Electroanal. Chem. 503 (1/2) (2001) 105–116.
[24] E.M. Genies, M. Lapkowski, J.F. Penneau, J. Electroanal. Chem. 249 (1988) 97–107.
[25] W.W. Focke, G.E. Wnek, Y. Wei, J. Phys. Chem. 91 (1987) 5813–5818.
[26] Y.G. Wang, Y.Y. Xia, J. Electrochem. Soc. 153 (2006) A450–A454.
[27] E. Frackowiak, S. Delpeux, K. Jurewicz, K. Szostak, D. Cazorla-Amoros, F. Beguin, Chem. Phys. Lett. 361 (2002) 35–41.